Comparison of Nonlinear Dynamic Analysis of Time History and Endurance Time Method in Tall Structures with Frame-Wall System

Mohammadizadeh, M.R.[1]* and Jafarzadeh, A.[2]

[1] Associate Professor, Department of Civil Engineering, University of Hormozgan, Bandar Abbas, Iran.
[2] M.Sc., Islamic Azad University, Bandar Abbas Branch, Bandar Abbas, Iran.

© University of Tehran 2021

ABSTRACT: In this study, the seismic response of tall concrete structures with a special dual frame-wall concrete system is investigated using the endurance time method, and the results are compared with nonlinear time history analysis results. For this purpose, first, appropriate analytical models including buildings with concrete framed-wall system and 20, 30, and 40 stories are modeled non-linearly in PERFORM 3D software, and then, main nonlinear time history analyses are carried out for seven ground motions (accelerogram) further from the fault based on the FEMA P695 code and the endurance time accelerogram of (in) series. The results of the analysis are compared using indices (shear, relative displacement, and acceleration). The results indicate that the endurance time method is accurate in two indices of shear and acceleration, but the accuracy of the relative displacement index of the floor decreases as the number of stories of the structure increases.

1. Introduction

The growth and development of new tall structures began in the 80s of the nineteenth century with commercial and residential applications. Structurally, a tall structure is one which its height imposes special considerations or a structure with a period of more than 0.7 seconds. Due to the high number of degrees of freedom and the complexity in the behavior of tall structures, the analysis of tall structures requires the methods that predict the actual behavior of these structures with acceptable accuracy and the least time possible. Endurance time method is a seismic analysis that allows engineers and researchers to obtain the most information from the state of the structures with the lowest computational cost. This warrants provision of a scientific documentation of the precision of this method in the field of seismic design of which unknowns and uncertainties are an integral part, in order to take a step towards the better introduction of this method. It is necessary to create a nonlinear model and to perform nonlinear analysis of the time history in order to design tall structures. Endurance time method can be used to reach more comprehensive responses in less

* Corresponding author E-mail: mrzmohammadizadeh@yahoo.com

time compared to the natural accelerogram method.

One of the most efficient lateral resistant systems used in tall structures is the wall frame system. In recent years, studies have been carried out on structures with a lateral resistant frame-wall system (Memari et al., 2000; Kim et al., 2007; Shin et al., 2010; PEER, 2010). Mali et al. (2010) have reported details of the nonlinear modeling of structures with lateral resistant concrete frame-wall system. Using the idea of the cardiac test, Estekanchi et al. (2004) presented the idea of endurance time method for the first time. Estekanchi et al. (2007) also showed the application of the endurance time method in seismic analysis within the linear range. In that research, the generation of acceleration functions related to the endurance time method and results of the modeling of multiple frame analysis were examined. Estekanchi et al. (2008) compared the failure indices in the methods of time histories and endurance time. Riyahi and Estekanchi (2010) compared the methods of time history and endurance time in the study of steel frames. Valamanesh and Estekanchi (2010) and Valamanesh (2010) presented a method for three-dimensional analysis using the time-endurance method and examined the accuracy of this method in the three-dimensional analysis of moment frames in the elastic range. Estekanchi et al. (2011) applied the endurance time method in seismic assessment of steel frames to examine the adequacy of this method for these structures.

Also, Foyouzat and Estekanchi (2016) examined concerning application of rigid-perfectly plastic spectra in improved seismic response assessment by the endurance time method which played a great role in strengthening and expanding it. For other investigations related to the endurance time method (one can refer to Basim and Estekanchi, 2015; He et al., 2015; Guo et al., 2016; Tafakori et al., 2017; Bai et al., 2019; Li et al., 2019; Seyed Kolbadi et al., 2020).

No research has been conducted yet to investigate the structural response using the endurance time method in tall structures. So, in this research, the seismic response of tall concrete structures with a lateral resistant frame-wall system using nonlinear analysis of time history and endurance time methods has been investigated. Therefore, the buildings with a special resistant moment frame system and shear core with 20, 30 and 40 stories including coupling shear wall in one direction are analyzed using the powerful 3D Perform software with 7 different accelerogram records. The buildings are designed in accordance with the ACI 318 (2014) regulations for specific norms and indices such as story drift, story shear and the acceleration of stories are calculated.

2. The Concept of the Endurance Time

The concept of the endurance time method can be excellently explained with a hypothetical experiment. For example, the structural performance of three different structures with unspecified characteristics is evaluated against earthquakes. In this evaluation, these three structures are placed on a shake table. The experiment begins with vibrational stimulation that intensifies as the time passes, and the structure response increases with the passage of time and subsequently the amplitude of the stimulation increases, and the state of the structure changes from linear and undamaged mode to a partial failure mode, to yield points of some components and ultimately reaches dynamic instability level subsequent to entering into the nonlinear region and increasing of the structure response amplitude.

The values of the failure indices can be graphed directly versus time, for example, the maximum relative displacement of the stories is plotted in Figure 1. As it can be seen, in general, the range of failure indices in frame A is higher than others and it is lower than the rest of them in frame B. As a result, it can be said that the performance of

the B structure is more favorable than the other two structures at different intensities. It is also possible to conclude from the response curves that frames A, C and B reach the failure mode after 8, 13 and 18 seconds, respectively.

As a result, regarding these time periods and the corresponding intensity of the structure stimulation, it is possible to achieve the extent of the failure of the structures and the maximum period of time that they are able to withstand the load imposed by increasing acceleration function. If these three structures are three different designs for one purpose and their performance level and the soil type of the region are the same, it can be concluded that the structure B has a more favorable performance than the other two structures. In this case, if the acceleration function is capable of meeting the requirements of the design in accordance with regulations, the target time can be set for a standard structure to be allowed to fail to the specific degree at that time. In the endurance time method, the incremental changes of acceleration are considered linear in time. In Figure 1a, the acceleration function-time graph is illustrated. As shown in Figure 1a, the duration of the acceleration function and its intensity increase over time. Figure 1b illustrates the behavior of the frames examined under increasing acceleration function and Figure 1c shows the response of different structures to this acceleration function in time.

3. Modeling and Design of Buildings

For the purpose of this study, three concrete buildings with a special dual resistant lateral system (the resistant lateral system includes a special moment frame with a shear wall, each able to withstand at least 25% and 50% of the earthquake load, respectively) are considered and the number of stories are selected to be 20, 30, and 40. In the design of these buildings, the ACI318-14 regulations have been used. The structures have been modeled in three dimensions and

analyzed through ETABS2016 software by spectral dynamic analysis using the 2800 Standard Design (2014) spectrum of Iran (to consider the effect of earthquake force). The 2800 standard design spectrum of Iran is illustrated in Figure 2.

In all buildings, the height of the stories is the same and equal to 3.4 meters, as shown in Figure 3. The dead and live loads distributed on the floors are considered to be 6 KN/m^2 and 2 KN/m^2, respectively. The characteristic strength of steel and concrete is considered to be F_y = 400 Mpa and F_c = 30 Mpa. Regarding the construction of buildings in areas with high relative risk, the acceleration coefficient of the design (A) is assumed to be (0.3). The experimental period is calculated from the following Eq. (1):

$$T = 0.05H^{3/4} \qquad (1)$$

where T and H: are period and height of the structure, respectively.

The soil of the region is assumed to be of type Ⅲ and the behavioral coefficient of the resistant lateral dual system is based on the fourth edition of the code for calculating earthquake load in Iran (the standard 2800). Therefore, the buildings are designed according to the regulations of the seismic design of the mentioned code. Tables 1-3 show the designed sections of different stories separately for each building.

4. Nonlinear Structural Modeling

In the nonlinear modeling of structures in the PERFORM software (Powell and Graham, 2011), the beam- column elements with joints on both ends of the element and fiber elements (referred to in ASCE41-13, 2013) have been used for elements of the beam, column and wall, respectively. In the modeling of wall elements, a combination of concrete and steel fibers (single-dimensional fiber threads) has been used, as shown in Figure 4. The number and distribution of fibers at the wall section must be optimized. It should be noted that

the use of few fibers or ones with inappropriate distribution cannot properly model the behavior of the wall.
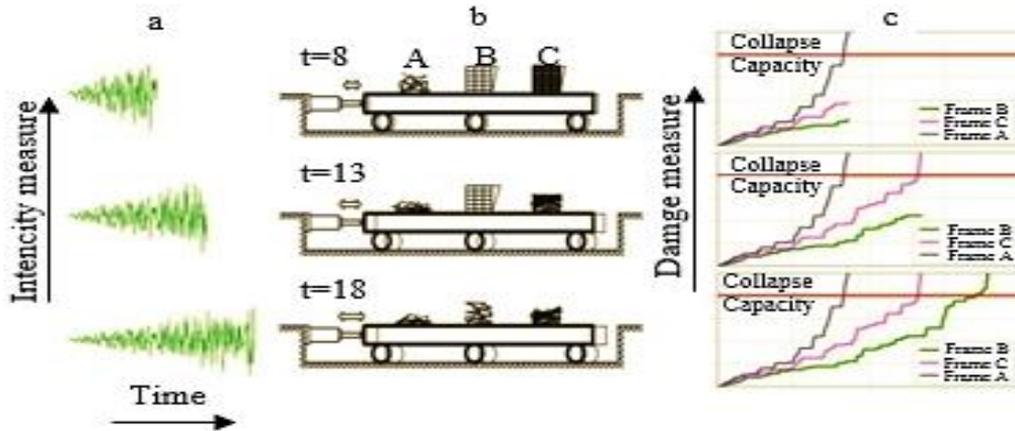
Fig. 1. The concept of endurance time in the form of hypothetical experiment (Valamanesh, 2010)
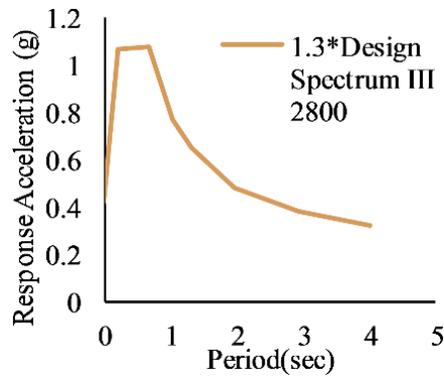
Fig. 2. The 2800 standard design spectrum (Standard 93-2800)
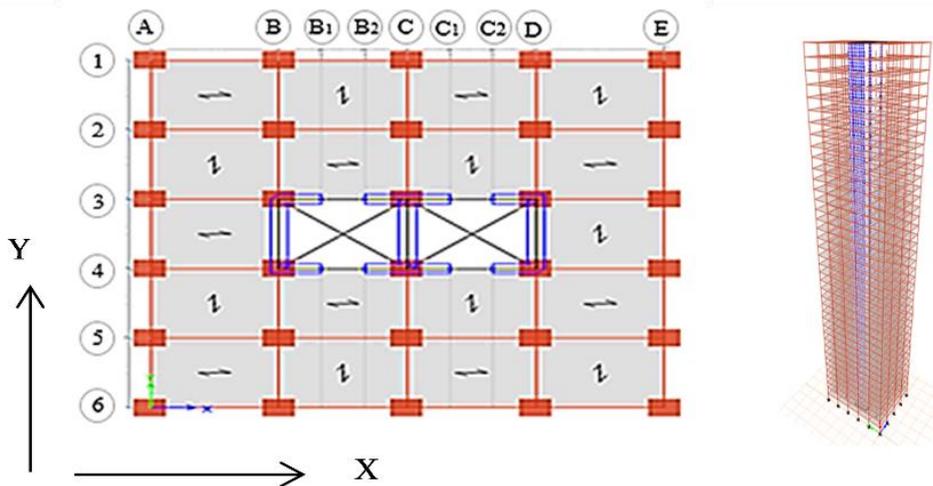
Fig. 3. Plans for buildings with 20, 30 and 40 stories as well as the 3D form

Table 1. Designed sections of the 20-story building

Story	Column			Beam			Beams Collector			Coupling			Wall
	ID	b	h	ID	b	h	ID	b	h	ID	b	h	
1-3	C95×95	95	95	B 60×80-1	80	60	CB 80×80-1	80	80	CPB 160×90-1	90	160	W60
4-6	C85×85	85	85	B 60×80-2	80	60	CB 80×80-2	80	80	CPB 160×90-2	90	160	W40
7-10	C70×70	70	70	B 60×60-1	60	60	CB 70×60-1	70	60	CPB 160×90-3	90	90	W30
11-14	C60×60	60	60	B 60×60-2	60	60	CB 70×60-2	70	60	CPB 150×60	60	60	W25-1
15-20	C50×50	50	50	B 60×50	60	50	CB 50×70	50	70	CPB 130×50	50	50	W25-2

Table 2. Designed sections of the 30-story building

Story	Column			Beam			Beams Collector			Coupling			Wall
	ID	b	h	ID	b	h	ID	b	h	ID	b	h	
1-3	C 110×110	110	110	B 70×90	90	70	CB 90×90	90	90	CPB 170×100	100	170	W70
4-7	C 95×95	95	95	B 60×80-1	80	60	CB 80×80-1	80	80	CPB 160×90-1	90	160	W60
8-12	C 85×85	85	85	B 60×80-2	80	60	CB 80×80-2	80	80	CPB 160×90-2	90	160	W40
13-18	C 70×70	70	70	B 60×60-1	60	60	CB 70×65-1	70	65	CPB 160×90-3	90	160	W30
19-24	C 65×65	65	65	B 60×60-2	60	60	CB 70×65-2	70	65	CPB 150×60	60	150	W25-1
25-30	C 50×50	50	50	B 60×50	60	50	CB 40×70	40	70	CPB 140×50	50	140	W25-2

Table 3. Designed sections of the 40-story building

Story	Column			Beam			Beams Collector			Coupling			Wall
	ID	b	h	ID	b	h	ID	b	h	ID	b	h	
1-3	C 150×150	150	150	B 100×100	100	100	CB 100×120-1	120	100	CPB 170×100-1	100	170	W80
4-8	C 135×135	135	135	B 90×90	90	90	CB 100×120-2	120	100	CPB 170×100-2	100	170	W70
9-14	C 115×115	115	115	B 70×90	90	70	CB 80×100-1	100	80	CPB 160×90-1	90	160	W60
15-20	C 95×95	95	95	B 60×80-1	80	60	CB 80×100-2	100	80	CPB 160×90-2	90	160	W50
21-26	C 85×85	85	85	B 60×80-2	80	60	CB 80×100-3	100	80	CPB 160×90-3	90	160	W40
27-32	C 70×70	70	70	B 60×60	60	60	CB 70×65	65	70	CPB 150×60	60	150	W30
33-40	C 55×55	55	55	B 60×50	60	50	CB 40×70	70	40	CPB 140×50	50	140	W25

On the other hand, the use of a large number of fibers increases the cost of computing. The behavior of the fibers is simulated using a model that is assigned as material properties (the stress-strain curve of fiber material) and in the center of each wall element. (Thomsen et al., 2004; Birely et al., 2008). Inelastic modeling of moment frame systems includes modeling for bending members (beam and column) and joints. In these types of systems, inelastic deformation should occur in bending joints in the beams and columns. It should be noticed that fulfilling the minimum code requirements does not necessarily prevent the creation of a plastic joint in the column and the nonlinear deformations of the connection area in the column-beam joints. Therefore, non-linear models should include the points mentioned above unless the demand to capacity ratio is small enough to prevent it from occurring.

Typically, the beam-column elements are modeled using a central joint or fiber section. Although the fiber model generally has the ability to more accurately model the initial non-linear cracking effects in concrete and the distribution of concrete yielding, its ability in describing the failure associated with the sliding of the reinforcing bar in concrete connections and the local buckling and failure of the rebar is limited. Plastic joint models are often more applicable to describe the general behavior of force-deformation (moment-rotation), including the strain softening. Modeling concrete frames that consider seismic design requirements is somewhat more difficult than steel frames. The hardness of members is affected by the cracking of the concrete. The beam-column connection is affected by the cracking of the concrete and the rebar slipping. The response is also sensitive to the axial force after reaching the yield point while the columns and connections enter the plastic region.

ASCE41-13 and PEER/ATC72 have developed models and recommendations for determining the stiffness of the members, the features of the nonlinear joint of the member, and strategies for connection modeling, which are outlined in the following. The structural model should be able to simulate structural failure and collapse of the structure when the structure is under severe earthquake. Determining crucial failures and collapse modes is a key factor in the selection of nonlinear

analytical model.

The general view of the generated model for a frame is as follows: A beam-column element with a central nonlinear rotational joint at each end and a beam-column connection with limited length using five non-linear centralized springs to model the shear failure of the connection plate and the sliding of the reinforcement bar in each side of the connection. The modeling is schematically illustrated in Figure 5.

Since the probability of failure in the beam and column of the concrete moment frame is higher, the accurate modeling of the inelastic effect in the beam-column elements is essential in the collapse modeling. The centralized joint is selected due to its simplicity and the inherent limitations of the fiber model (using a fiber model in the simulation of the strain softening associated with the rebar buckling is difficult).

The fiber model represents the distribution of plasticity along the member and modeling can be done so that it stimulates the behavior caused by concrete failure from the initiation of the crack to concrete breakage. However, the existing steel models do not have the ability to represent the buckling behavior and the rebar failure. Because of such limitations, the available fiber model is not adequate enough to simulate the collapse. Despite the fact that a centralized joint model does not have the accuracy of the fiber model, it can be calibrated in such a way that it shows the failure issued from the buckling of the rebar and the failure of the rebar stirrup and results in the loss of concrete confinement (Mander et al., 1988).
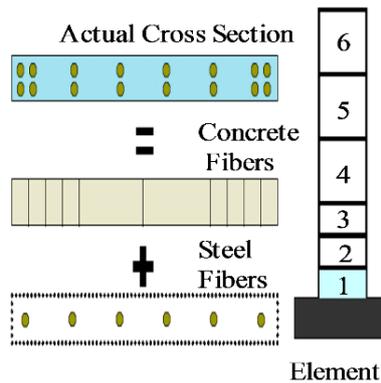
Fig. 4. Fiber modeling shear wall elements (PEER, 2010)
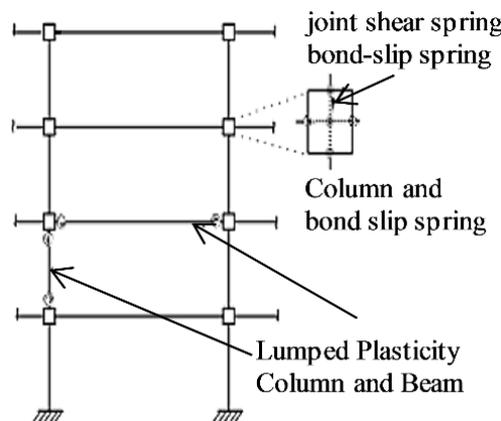
Fig. 5. Schematic representation of frame construction members (FEMA P695, 2009)
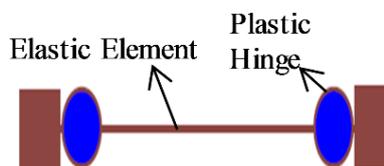
Fig. 6. Simple form of plastic joint (Hasleton et al., 2008)

Figure 6 depicts a simple view of a centralized joint model, and Figure 7 illustrates the moment-rotation behavior of the plastic joint. This model is composed of an elastic element with two plastic joints on both ends. The parameters required for defining the plastic joint behavior (Figure 7) include elastic hardness e_k, yield moment M_y, ultimate moment M_c, plastic rotation originated from the ultimate moment θ_{cap}^{pl}, and slope of the strain softening region K_c, which have been illustrated in Figure 7.

Eq. (2) has been developed and calibrated in order to obtain the yield moment of concrete member (Hasleton and Deierlein, 2007).

$$
\begin{aligned}
\frac{M_y}{bd^3} = \varphi_y \Bigg(E_c * \frac{\xi^2}{2}\left(\frac{1+\delta'}{2} - \frac{\xi_y}{3}\right) \\
+ \frac{E_S(1-\delta)}{2}\Big[(-\xi_y)\rho_1 \\
+ (\xi_y - \delta')\rho_2 \\
+ \frac{\rho_v}{6}(1-\delta')\Big]\Bigg)
\end{aligned}
$$

$$\alpha = \frac{E_S}{E_C} \quad \xi_y = (\alpha^2 A^2 + 2\alpha B)^{\frac{1}{2}} - \alpha A \quad \varphi_y =$$

$$\frac{f_{y1}}{E_S(1-\xi_y)d} \quad \rho_1 = \frac{A_s}{bd} \quad \rho_2 = \frac{A_s'}{bd} \quad \rho_v = \frac{A_{sw}}{bd}$$

$$s' = \frac{d'}{d} \quad B = \rho_1 + \delta'\rho_2 + \frac{\rho_v(1+\delta')}{2} +$$

$$\frac{N}{bd f_{y1}} \quad A = \rho_1 + \rho_2' + \rho_v + \frac{N}{bd f_{y1}}$$

$$(2)$$

where M_y: is the single-axial yield moment, φ_y: is the yield curvature, f_{y1}: is the yield stress of tensile rebar, ε_y: is the neutral axis depth in yield, d': is the distance between the centroid of the steel under compression and the farthest compression fiber of section, N: is the axial load (positive in compression), α: is the modulus of elasticity coefficient, d: is the effective depth of section and b: is the compression flange width.

The hardness of the hardening region will be obtained after yield point by division of the maximum ultimate moment to the yield moment (Eq. (3)). Researches suggest that the hardening ratio depends on the axial force and tensile rebar ratio. According to Haselton et al. (2007), the ratio of the axial load and concrete strength are among the key factors in determination of the hardness ratio.

$$\frac{M_C}{M_y} = (1.25)(0.89)^v(0.91)^{0.01 f_c'} \qquad (3)$$

where M_C and M_y: are the maximum moment capacity and yield moment capacity, respectively.

Eq. (4) is presented for estimation of the plastic rotational capacity.

$$
\begin{aligned}
\theta_{cap,pl} \\
= 0.12(+0.55 a_{sl})(0.16)^v(0.0 \\
+ 40\rho_{sh})^{0.43} \\
* (0.54)^{0.01 f_c'}(0.66)^{0.1 S_n}(2.27)^{10\rho}
\end{aligned}
\qquad (4)
$$

where a_{sl}: is the probability of the rebar slipping, so that the zero value is considered impossible and the value of 1 is considered as possible for the above phenomenon. ρ_{sh} and ρ: are percentages of the longitudinal and transverse rebar, respectively and v: denotes the axial load ratio.

In spite of the importance of the parameter θ_{pc} in estimating the collapse capacity, the amount of research carried out regarding its estimation is inadequate. The important parameters in the calculation of θ_{pc} are the axial load ratio v and the transverse rebar ratio ρ_{sh}. In Eq. (5) the upper limit imposed by the lack of information is reliable. However, it may be rigorous for well-confined members.

$$
\begin{aligned}
\theta_{pc} = 0.76(0.031)^\vartheta(0.02 \\
+ 40\rho_{sh})^{1.02} \le 0.1
\end{aligned}
\qquad (5)
$$

Nonlinear modeling parameters can be obtained by using laboratory results or by using the ASCE41-13. In the case of using the ASCE41-13 code, the rotation capacity of the member is obtained by two parameters of a and b. In Figure 8, the a and b parameters are a part of the deformation that occurs after the yield point and are referred to as plastic deformations. These parameters can be acquired using the

ASCE41-13.

The rotational capacity of the members is determined on the basis of the curvature capacity of the cross section and the length of the plastic joint. Such that, using the moment-curve analysis, the curvature corresponding to the yield point and ultimate curvature of the cross section are determined, and using the length of the plastic joint, the rotational capacity of the member is obtained.
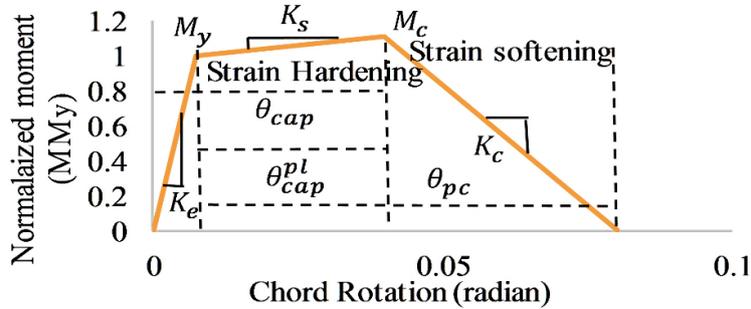
Fig. 7. Monotonic behavior of component model (FEMA P695, 2009)
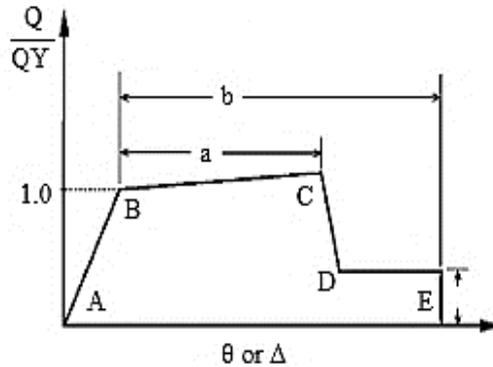
Fig. 8. The Force-Deformation of members' model (FEMA356, 2000)
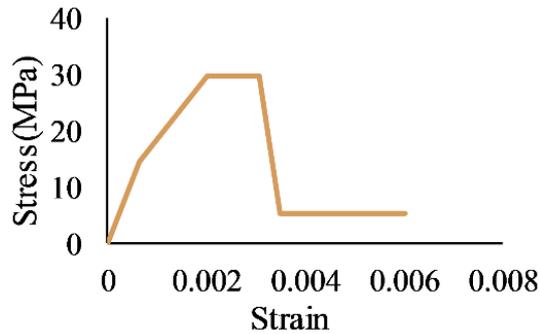
Fig. 9. Modeling of concrete behavior in software
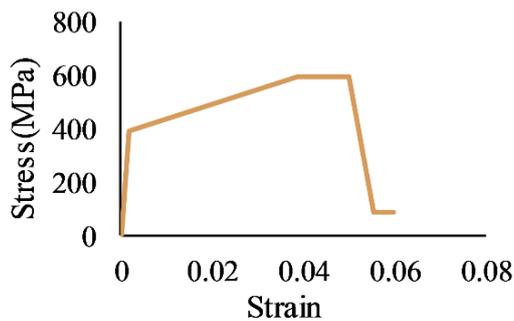
Fig. 10. Modeling of steel in behavior software

For the modeling of shear walls, it is necessary to introduce the stress-strain curves of steel and concrete. Therefore, the stress-strain curves of steel and concrete are shown in Figures 9 and 10, respectively.

5. Employed Accelerograms and Their Scaling Procedure

In this study, seven accelerations of the FEMA-P695 have been used, as given in Table 4, which are acquired from the PEER website. The fourth edition of Iran's 2800 standard is used as follows in order to scale the records.

5.1. Scaling of the Endurance Time Functions

In this study, the ETA20 in records of the endurance time function have been used for the non-linear analysis of the structures on hard soil types (FEMA P695, 2009). The spectrum of acceleration for 0 to 12 seconds of each pair of the functions is calculated separately, and the spectra of the square root of sum of squares is computed to scale the endurance time functions at hazard level 1. Then, to each of these three spectra, a scale coefficient is assigned in such a way that the area under them in the interval of 0.2 to 1.5 times the first vibrational mode period of the structure becomes equal to the area of the target spectrum. The target spectrum for scaling is considered to be the SRSS average spectrum of the acceleration spectra of the scaled natural accelerogram (7 records) at hazard level 1, for the main period of the structure. In the following, first, the SRSS of the response spectrum for three pairs of the scaled endurance time functions is obtained. Then, for each structure, the average response spectrum is obtained based on the target time, which is different for each structure.

Figures 11a-11c illustrate the comparison of the SRSS average response spectrum of the 7 scaled records (target spectrum) with the SRSS average spectrum of the scaled endurance time spectrum for structures of 20, 30 and 40 stories,

respectively. Using the trial and error procedure, the target time for the 20, 30, and 40-story structures is calculated to be 12, 15, and 19 seconds, respectively. Because the target time of 12 seconds has been used for all of the structures, therefore, some scale coefficients should be used to match the response spectrum obtained from the endurance time method, for each structure with the target spectrum. These calculated coefficients are presented in Table 5.

6. Comparison of the Results of the Two Methods

In this section, the results related to drift of the stories (relative displacement of stories) as well as shear and acceleration of the stories have been examined based on the results of nonlinear analysis. The vertical axis shows the number of stories and the horizontal axis represents the maximum drift of stories (the average of the maximum drift responses of the 7 records is selected by the FEMA-P695). The comparison of maximum drift in the x, y directions for structures with 20, 30, and 40 stories is indicated in Figures 12-13, using both methods of time history analysis and the endurance time analysis, respectively. By comparing the results, it can be seen that by increasing the number of stories, the drift error of the stories will increase by about 20%. By comparing Figures 14 and 15, it can be seen that the acceleration error rate is 13, 15 and 15 percent in the structures of 20, 30 and 40 stories, respectively. The relative error in estimating the acceleration of stories in the endurance time method and time history analysis method does not change with elevation of the structure and the results of the two methods correspond to each other. Figures 16 and 17 illustrate the average of the results obtained in the 12th second of the nonlinear endurance time analysis for story shear, which is very consistent with the results of the nonlinear time-history analysis method, and with increasing the height of the structure, the accuracy of this method is not diminished.

Table 4. Records employed in this study (FEMA P695, 2009)

ID No.			PEER-NGA record information		Recorded motions	
	Rec. Sec	Lowest freq. (HZ)	File names-horizontal records		PGA (g)	PGV (cm/s)
1	767	0.13	RSN752_LOMAP_CAP000	RSN752_LOMAP_CAP090	0.53	35
2	1633	0.13	RSN1633_MANJIL_ABBAR-L	RSN1633_MANJIL_ABBAR-T	0.51	54
3	953	0.25	RSN953_NORTHR_MUL009	RSN953_NORTHR_MUL279	0.52	63
4	1787	0.04	RSN1787_HECTOR_HEC000	RSN1787_HECTOR_HEC090	0.34	42
5	1111	0.13	RSN1111_KOBE_NIS000	RSN1111_KOBE_NIS090	0.51	17
6	1485	0.05	RSN1485_CHICHI_TCU045-E	RSN1485_CHICHI_TCU045-N	0.44	115
7	1158	0.24	RSN1158_KOCAELI_DZC180	RSN1158_KOCAELI_DZC270	0.36	59

Table 5. Scale coefficients of the endurance time functions with SRSS average of the 7 scaled records

Record name	Scale factor 20 story	Scale factor 30 story	Scale factor 40 story
ETA20inx01	0.99	1.276	1.903
ETA20iny01	0.99	1.276	1.903
ETA20inx02	1.05	1.268	1.834
ETA20iny02	1.05	1.268	1.834
ETA20inX03	1.04	1.328	1.98
ETA20iny03	1.04	1.328	1.98
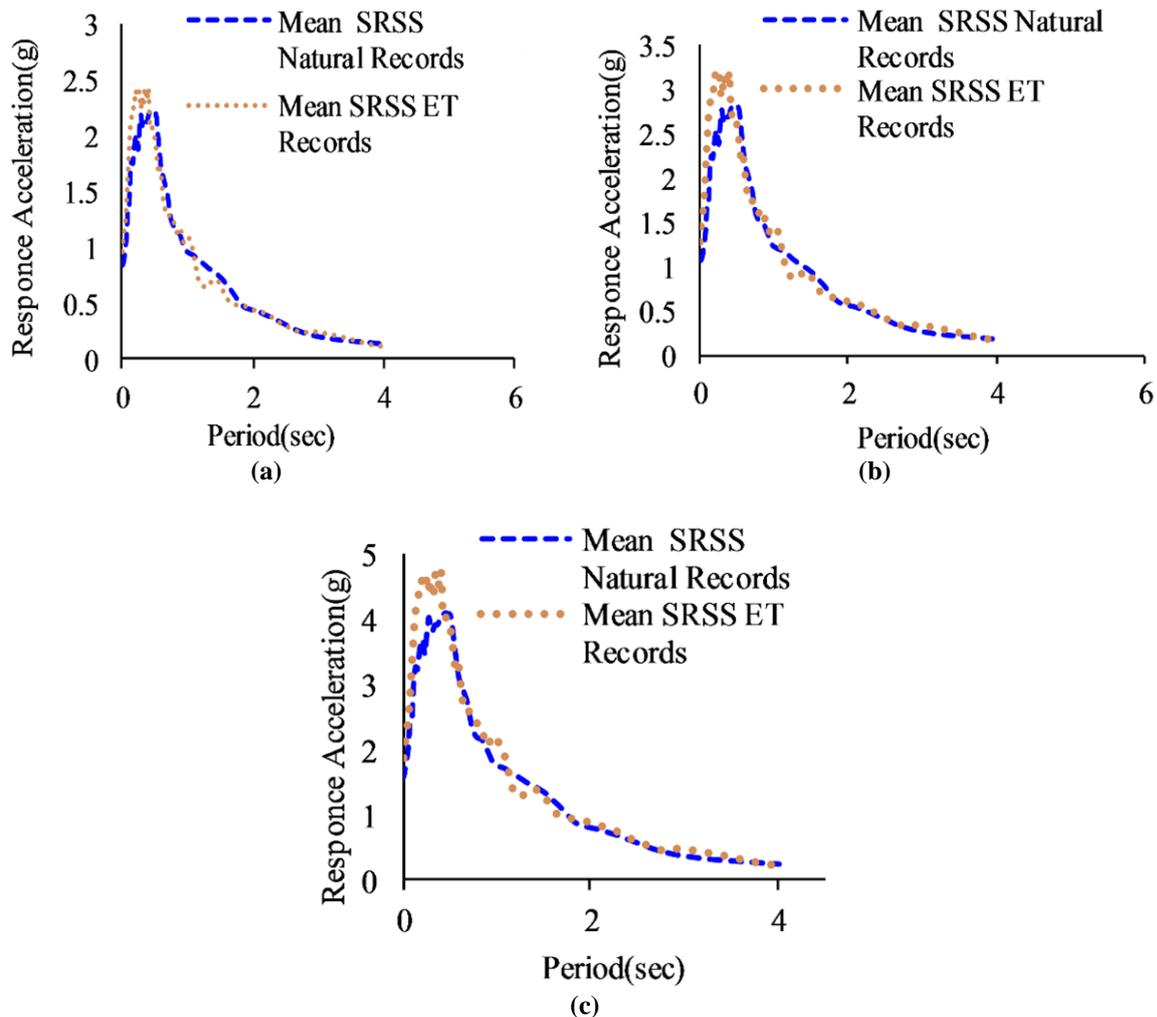
Fig. 11. Scaling of the endurance time functions with the average of the 7 scaled natural records for: a) 20-story; b) 30-story; and c) 40-story structure
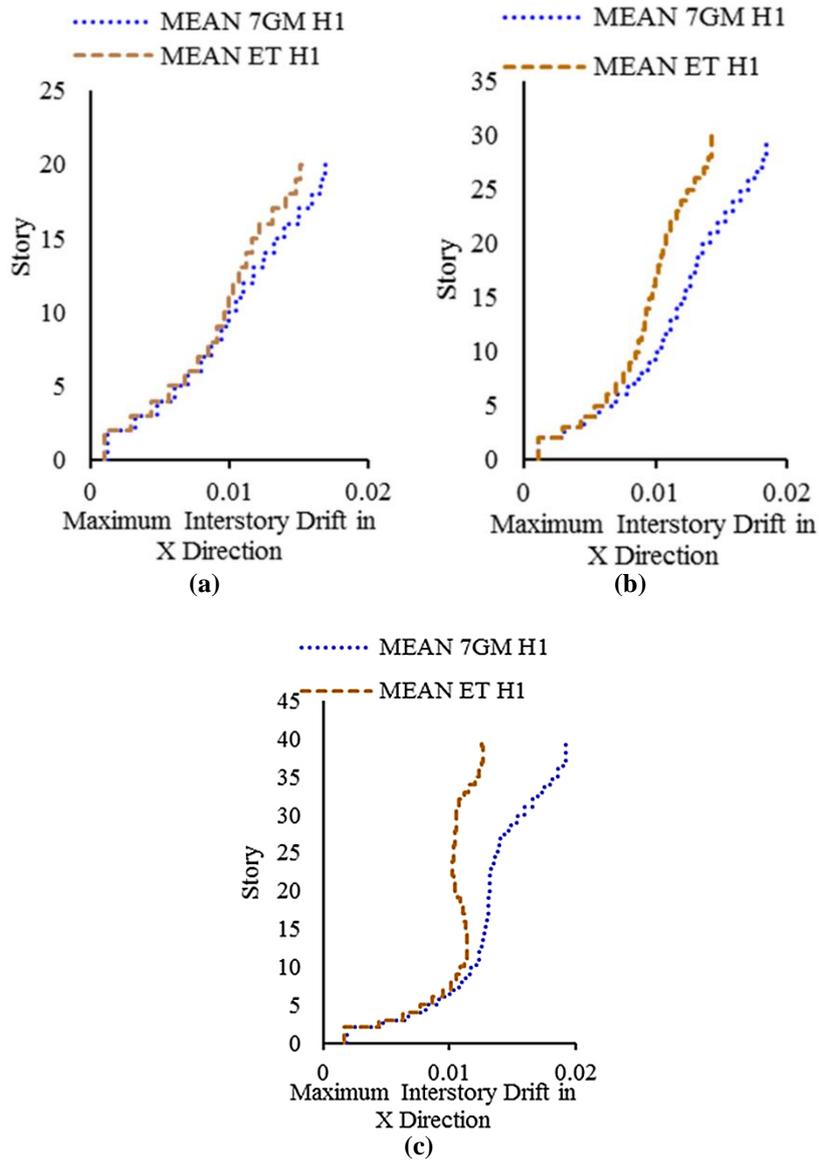
Fig. 12. Story drift in the X direction- Nonlinear time history analysis- 12th second of the endurance time for: a) 20-story; b) 30-story; and c) 40-story

(c)
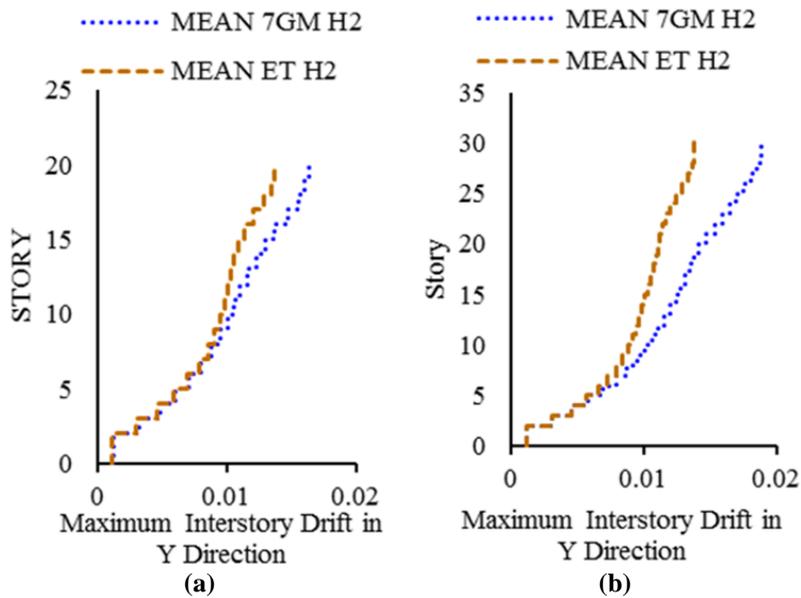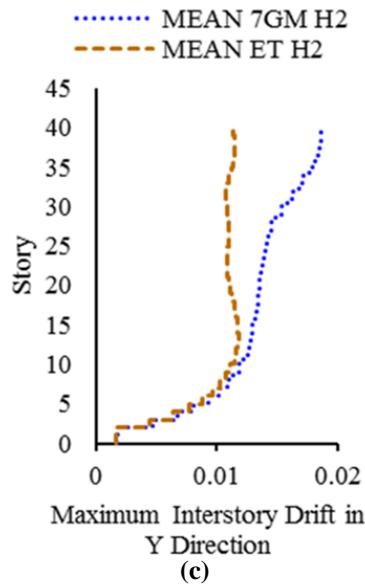
Fig. 13. Story drift in the Y direction- Nonlinear time history analysis 12th second of the endurance time for: a) 20-story; b) 30-story; and c) 40- story

(a)

(b)

(c)
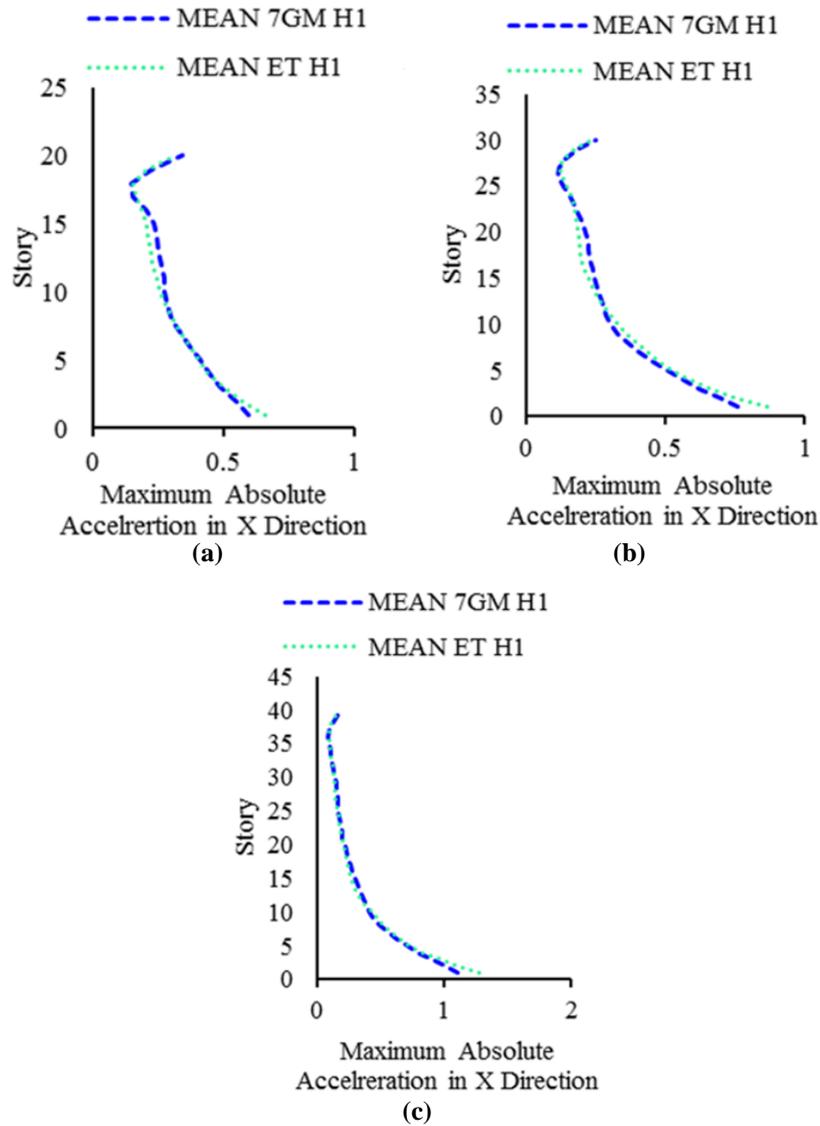
Fig. 14. Absolute acceleration in the X direction- Nonlinear time history analysis 12th second of the endurance time for: a) 20-story; b) 30-story; and c) 40-story
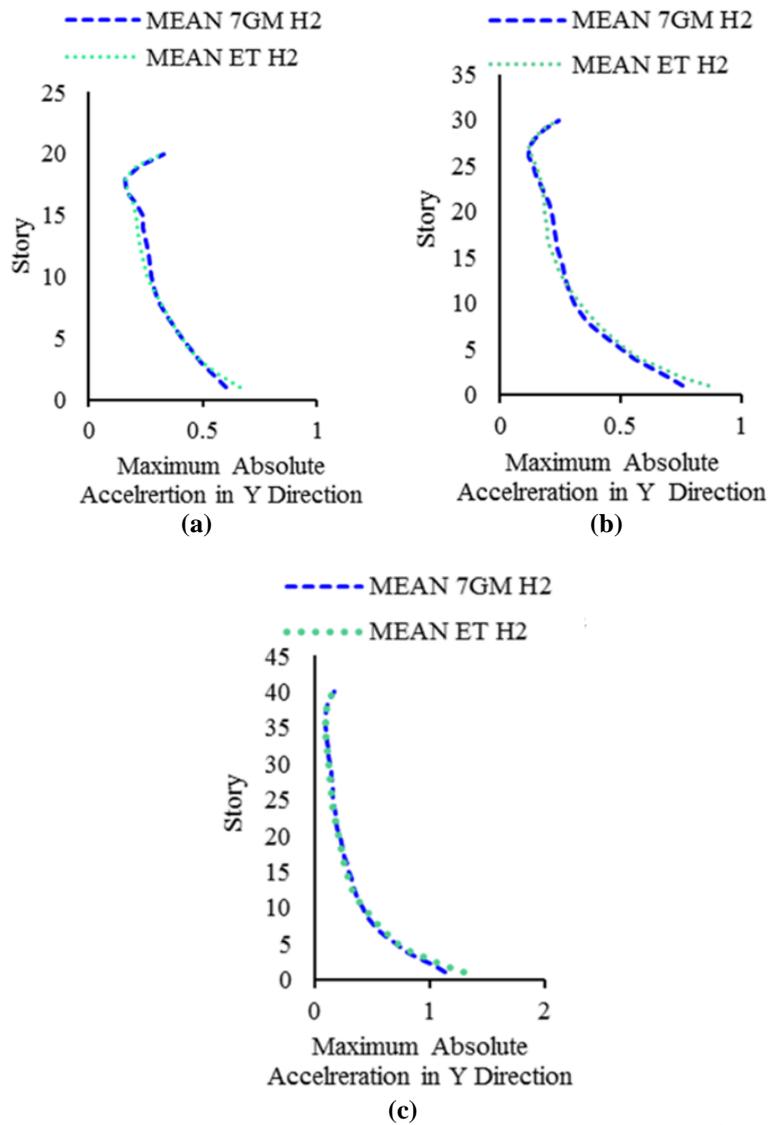
Fig. 15. Absolute acceleration in the Y direction- Nonlinear time history analysis 12th second of the endurance time for: a) 20-story; b) 30-story; and c) 40-story

(c)
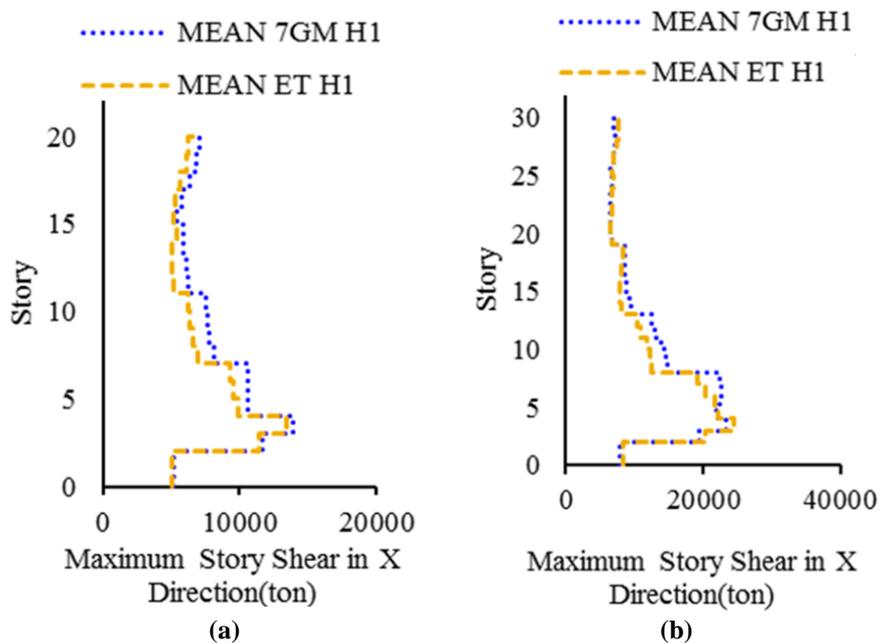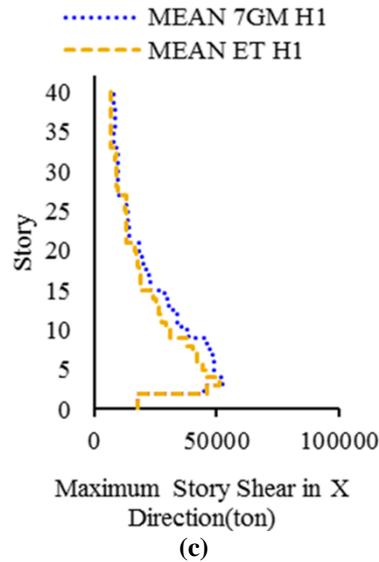
Fig. 16. Story shear in the X direction- Nonlinear time history analysis 12th second of the endurance time for: a) 20-story; b) 30-story; and c) 40-story

(a)

(b)

(c)
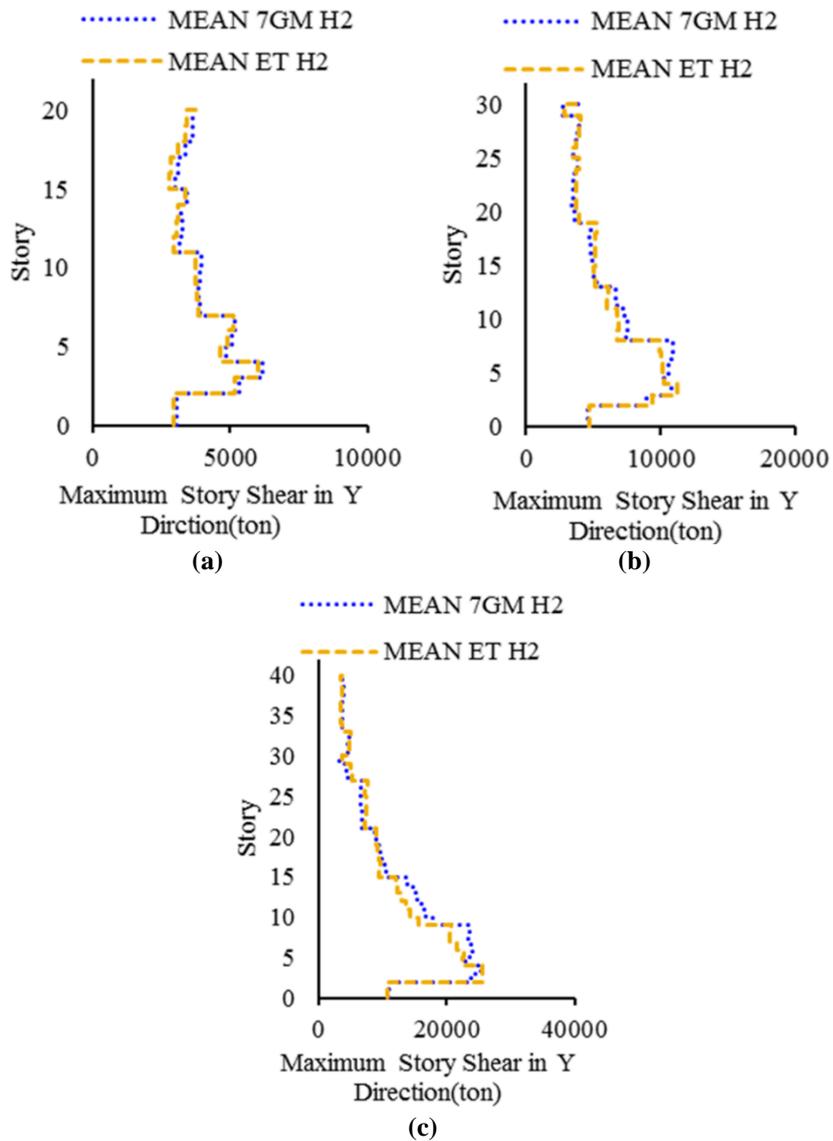
Fig. 17. Story shear in the Y direction- Nonlinear time history analysis 12th second of the endurance time for: a) 20-story; b) 30-story; and c) 40-story

7. Relative Error Analysis of the Endurance Time Method

In this research, three structural models for 20, 30 and 40 story-structures were investigated. The average of maximum responses (drift, shear and acceleration) of the buildings with different heights according to the results obtained from Figures 12-17 are presented in Table 6, in order to recapitulate the results. This table indicates the maximum error ratio of the endurance time method to the nonlinear time history analysis of the studied structures. The error rate of the two responses of shear and acceleration does not change much with the increase of the period of the structure, but the accuracy of the drift response is diminished. It seems that by reforming the records (which leads to an increase in the spectrum acceleration of the artificial records), it is possible to improve the accuracy of the story drift response in higher periods.

7.1. Comparison of Analysis Time in Endurance Time Methods and Nonlinear Time History

With regard to this matter that in tall structures with a large number of floors, the number of degrees of freedom increases significantly, so the analysis time using the time history method will be very long. One of the advantages of the endurance time method is the reduction of the analysis time compared to the time history method. In Table 7, the analysis time of a 20-story structure has been compared with the relevant earthquake accelerograms using endurance time and time history methods. The results show that the time of analysis in the endurance time method has a significant reduction compared to the time history method. The processor system related to the computer which the analyzes were performed, is Intel® Dou Core ™ 2, CPU 2.2 GHZ, 3GB RAM.

8. Conclusions

In this research, concrete frames with special dual structural system and different heights using PERFORM software were analyzed by two methods of endurance time and time history. In the analysis procedure, the geometric and material nonlinearities were taken into consideration. Comparing the results of the two methods, the following general results are obtained.

Table 6. Maximum relative error of the endurance time analysis method compared to the time history analysis method (percent)

Story shear		Absolute acceleration		Story drift		Indices
Y	X	Y	X	Y	X	structure
9	18	12.5	13	18	13	20 STORY
11	17	20	15	27	27	30 STORY
15	19	15	15	39	34	40 STORY

Table 7. Records analysis time

ID No.	File names-Horizontal records		Time(s) records	Time step	Analysis time (min)
1	RSN752_LOMAP_CAP000	RSN752_LOMAP_CAP090	39.99	0.005	400
2	RSN1633_MANJIL_ABBAR--L	RSN1633_MANJIL_ABBAR--T	53.5	0.02	135
3	RSN953_NORTHR_MUL009	RSN953_NORTHR_MUL279	29.98	0.01	150
4	RSN1787_HECTOR_HEC000	RSN1787_HECTOR_HEC090	45.3	0.01	230
5	RSN1111_KOBE_NIS000	RSN1111_KOBE_NIS090	40.95	0.01	200
6	RSN1485_CHICHI_TCU045-E	RSN1485_CHICHI_TCU045-N	89.995	0.005	900
7	RSN1158_KOCAELI_DZC180	RSN1158_KOCAELI_DZC270	27.18	0.005	325
8	ETA12inx01	ETA12iny01	12	0.01	75
9	ETA12inx02	ETA12iny02	12	0.01	75
10	ETA12inx03	ETA12iny03	12	0.01	75

- The results of the endurance time analysis on the overall behavior of the structure (drift, shear, and acceleration of stories) are in most cases in the range of minus one to plus one a standard deviation from the average of time history analysis and the maximum average error percentage of the endurance time method to the time history method for buildings of 20, 30 and 40 stories is 18, 27 and 39 percent, respectively.

- According to the results of the acceleration and shear responses for buildings with different heights, the difference between the results of the two methods of endurance time and time history is almost constant, which indicates the independence of the accuracy of the endurance time method from the seismic intensity and type of the analysis.

- Comparison of the story drifts calculated by nonlinear time history method indicates that with respect to the studied structures, the relative accuracy of the method is reduced by increasing the height of the structure. As the height of the structure increases, the period of the structure is increased. This can be due to the generation of series (in) records with mostly low frequency periods, which can be improved by generating appropriate records for drift response and tall structures.

9. References

ACI 318. (2014). "Building code requirements for structural concrete and commentary", American Concrete Institute, Farmington Hills, MI, USA.

American Society of Civil Engineers (ASCE). (2013). "Standard ASCE/SEI 41-13, Seismic evaluation and retrofit of existing buildings", Reston, Virginia, U.S.A.

Bai, J., Jin, S., Zhao, J. and Sun, B. (2019). "Seismic performance evaluation of soil-foundation-reinforced concrete frame systems by endurance time method", *Soil Dynamics and Earthquake Engineering*, 118, 47-51.

Basim, M.C. and Estekanchi, H.E. (2015). "Application endurance time method in performance-based optimum design of

structures", *Structural Safety*, 56, 52-67.

Birely, A., Lehman, D., Lowes, L., Kuchma, D., Hart, C. and Marley, K. (2008). "Investigation of the seismic behavior and analysis of reinforced concrete structural walls", *Proceedings of the 14th World Conference on Earthquake Engineering*, Beijing, China.

Estekanchi, H.E., Vafaei, A. and Sadeghazar, M. (2004). "Endurance time method for seismic analysis and design of structures", *Scientia Iranica,* 11(4), 361-370

Estekanchi, H.E., Valamanesh, V. and Vafai, A. (2007). "Application of endurance time method in linear seismic analysis", *Engineering Structures*, 29(10), 2551-2562.

Estekanchi, H.E., Arjomandi, K. and Vafai, A. (2008). "Estimating structural damage of steel moment frames by endurance time method", *Journal of Constructional Steel Research*, 64(2), 145-155.

Estekanchi H.E., Riahi H.T. and Vafai A. (2011). "Application of endurance time method in seismic assessment of steel frames", *Engineering Structures*, 33(9), 2535-2546

FEMA. (2000). "Prestandard and commentary for the seismic rehabilitation of buildings", Federal Emergency Management Agency, Report FEMA-356, Washington, DC.

FEMA P695. (2009). "Quantification of building seismic performance factors", Applied Technology Council and Federal Emergency Management Agency, US.

Foyouzat M.A. and Estekanchi H.E. (2016). "Application of rigid-perfectly plastic spectra in improved seismic response assessment by Endurance Time method", *Engineering Structures*, 111, 24-35.

Guo, A., Shen, Y., Bai, J. and Li, H. (2017). "Application of the endurance time method to the seismic analysis and evaluation of highway bridges considering pounding effects", *Engineering Structures*, 131, 220-230.

Haselton, C.B., Goulet, C.A., Mitrani-Reiser, J., Beck, J.L., Deierlein, G.G., Porter, K.A., Stewart, J.P. and Taciroglu, E. (2008). "An assessment to benchmark the seismic performance of a code-conforming reinforced-concrete moment-frame building", PEER Report, 2007/1, Pacific Earthquake Engineering Research Center, Berkeley, CA.

Haselton, C.B., Deierlein, G.G. (2007). "Assessing seismic collapse safety of modern reinforced concrete moment frame buildings", John A. Blume Earthquake Engineering Center Technical Report 156, Stanford University.

He, H., Wei, K., Zhang, J. and Qin, S. (2015). "Application endurance time method to seismic fragility evaluation of highway bridges considering scour effect", *Oil Dynamics and Earthquake Engineering*, 136, 106243.

Kim, T. and Foutch, D.A. (2007). "Application of FEMA methodology to RC shear wall buildings governed by flexure", *Engineering Structures*, 29(10), 2514-2522.

Li, S., Liu, K., Liu, X., Zhai, C. and Xie, F. (2019). "Efficient structural seismic performance evaluation method using improved endurance time analysis", *Earthquake Engineering and Engineering Vibration*, 18(4), 795-809.

Malley, J.O., Dierlein, G., Krawinkler, H., Maffei, J., Pourzanjani, M., Wallace, J. and Heintz, J. (2010). "Modeling and acceptance criteria for seismic design and analysis of tall buildings", Applied Technology Council, PEER/ATC-72-1.

Mander, J.B., Priestley, M.J.N. and Park, R. (1988). "Theoretical stress-strain model for confined concrete", *Journal of Structural Engineering*, 114(8), 1804-1826.

Memari, A.M., Motlagh, A.Y. and Scanlon C, A. (2000). "Seismic evaluation of an existing reinforced concrete framed tube building based on inelastic dynamic analysis", *Engineering Structures*, 22(6), 621-637.

PEER. (2010). "Guidelines for performance-based seismic design of tall buildings", Pacific Earthquake Engineering Research Center, College of Engineering, University of California, Berkeley, USA.

PERFORM, C. (2011). *3D user manual (v5. 0.1)*, Berkeley, CA: Computer and Structures Inc, USA.

Riahi, H.T. and Estekanchi, H.E. (2010). "Seismic assessment of steel frames with the endurance time method", *Journal of Constructional Steel Research*, 66(6), 780-792.

Shin, M., Kang, T.H.K. and Grossman, J.S. (2010). "Practical modelling of high-rise dual systems with reinforced concrete slab-column frames", *The Structural Design of Tall and Special Buildings*, 19(7), 728-749.

Standing Committee on the Revision of the Regulations for the Design of Buildings against Earthquake. (2014). "Building regulations for building against earthquake", Standard 93-2800, Tehran, Iran.

Seyed Kolbadi, S.M., Piri, H., Keyhani, A., Seyed Kolbadi, S.M. and Mirtaheri, M. (2020), "Nonlinear seismic performance evaluation of flexural slotted connection using endurance time method", *Shock and Vibration*, 2020(4), 1-15.

Tafakori, E., Pourzeynali, S. and Estekanchi, H.E. (2017). "Probabilistic seismic loss estimation via endurance time method", *Earthquake Engineering and Engineering Vibration*, 16(1), 233, 245.

Thomsen IV, J.H. and Wallace, J.W. (2004). "Displacement-based design of slender reinforced concrete structural walls experimental verification". *Journal of structural engineering*, 130(4), 618-630.

Valamanesh, V. and Estekanchi, H.E. (2010). "A study of endurance time method in the analysis of elastic moment frames under three-directional seismic loading", *Asian Journal of Civil Engineering (Building and Housing)*, 11(5), 543-562.

Valamanesh, V. (2010). "3D nonlinear seismic analysis of structures by endurance time method", Ph.D. Thesis, Faculty of Civil Engineering, Sharif University of Technology, Tehran, Iran.